JOURNAL OF MATERIALS SCIENCE 17 (1982) 2625–2636

Liquid jet impact damage on zinc sulphide

S. VAN DER ZWAAG*, J. E. FIELD
Cavendish Laboratory, Madingley Road, Cambridge, UK

Zinc sulphide is an important infra-red transparent "window" material. When used in forward-facing aircraft components, these windows can be damaged by the impact of rain drops. The drop impact is simulated using a high-velocity jet technique and the resulting damage is described quantitatively and qualitatively for impact velocities up to 600 m sec^{-1}. For the 0.8 mm jets used, which simulate 4 mm diameter drop impacts, no loss of strength was observed for impacts at or below 125 m sec^{-1}. The calculated threshold velocity for a 2 mm drop impact of 175 ± 5 m sec^{-1} agrees well with results obtained on whirling-arm installations. Visual examination of the impact damage emphasized the importance of careful specimen preparation.

1. Introduction

Infra-red transparent materials are required in a wide range of optical systems where they are used for imaging (e.g. germanium lenses) or to protect electro-optical devices from the environment (e.g. zinc sulphide windows). The material requirements depend on the application but generally include low transmission losses, suitable refractive index, good mechanical strength and toughness, thermal and chemical stability, and erosion resistance. Furthermore, since these materials are used in imaging systems their optical properties should be isotropic.

Of particular interest are materials which are transparent in the 8 to 13 μm region, since this is the optimum wavelength for detecting and imaging objects with temperatures close to that of their background [1]. The range of materials with good transparency in this region includes only brittle materials such as chalcogenide glasses and some crystalline alkali-halides, sulphides, selenides, tellurides, arsenides and borides [1–4]. Because of the required optical isotropy only compounds with a cubic crystal structure can be used. At present the best combination of required properties is found in hot-pressed or chemical vapour deposited (CVD) zinc sulphide and zinc selenide which are both transparent in the visible as well as the infra-red part of the spectrum. The zinc sulphide has better mechanical properties but its transmission losses are higher than those of zinc selenide in particular in the visible and far infra-red part of the spectrum.

When brittle materials are used in forward-facing aircraft components they may suffer damage due to impact with rain drops. The damage is in the form of overlapping cracks which propagate along conical paths into the bulk of the specimen (analogous to Hertzian cone cracks). The cracks are detrimental since they not only reduce the transparency of the window but also cause strength reduction. In the present work the high velocity rain drop impact was simulated by firing a liquid jet at a stationary zinc sulphide specimen using the jet technique originally developed by Bowden and Brunton [5]. The jet impact damage was examined both quantitatively and qualitatively for impact velocities in the range 100 to 600 m sec^{-1}.

2. Experimental procedure

2.1. Material description

The zinc sulphide specimens available were produced by Raytheon Corporation using a CVD process. The specimens were translucent with a milky-yellow colour. Due to the "pebble" structure which forms during deposition, local fluctuations in the transparency (Fig. 1) are present. Large differences in size and intensity of the "pebble" structure were observed between individual specimens. Etching of the specimens in a

*Present address: Department of Metallurgy, Technical University Delft, Delft, The Netherlands.

0022–2461/82/092625–12$03.94/0

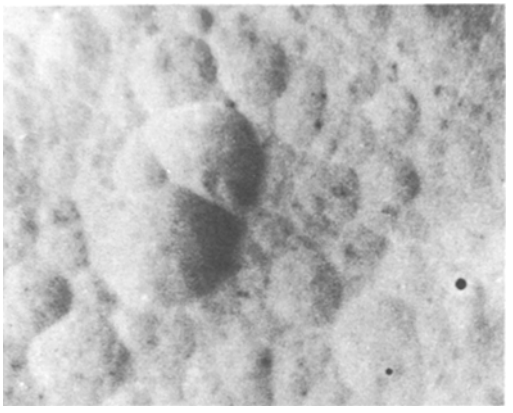

Figure 1 Optical transmission micrograph of the "pebble" structure below the surface (width of field 12 mm).

bromine–methanol solution (1:20 by volume) revealed a columnar grain structure. The axes of the columnar grains were normal to the specimen surface, i.e. normal to the plane of deposition. The average grain dimensions were 2 μm × 2 μm × 25 μm and the variation in grain size was small.

Detailed X-ray reflection measurements have revealed a well-defined texture of an (100) nature i.e. for most crystals the ⟨100⟩ direction is normal to the surface of the specimen and hence parallel to the axes of the columnar grains. No preferential orientation of the crystals in the plane of the surface could be detected. The sharpness of the Debye–Scherrer rings and that of the reflection peaks indicated the absence of large internal stresses.

The composition of the CVD zinc sulphide specimens was determined by X-ray microanalysis (Applied Research Laboratory electron microprobe microanalyser with X-ray spectrometers) and was stoichiometric.

The critical stress intensity factor, K_{Ic}, was measured using the Vickers indentation technique developed by Lawn and Fuller [6]. The average value determined was $K_{Ic} = 0.75 \pm 0.05$ M Nm$^{-3/2}$ (fracture surface energy = 3.4 Jm^{-2}). This result agrees well with those reported in the literature ($K_{Ic} = 1.0$ M Nm$^{-3/2}$, double torsion technique [7]; $K_{Ic} = 0.69$ M Nm$^{-3/2}$, double cantilever technique [8]; $K_{Ic} = 0.67$ M Nm$^{-3/2}$, four-point bending technique [9]).

2.2. Liquid jet impact

In the liquid jet technique, a lead slug is fired with a 0.22 calibre air-rifle into the rear of a water-filled stainless steel nozzle. The forward motion of the sealing neoprene disc extrudes the water at high velocity through a narrow orifice section at the front of the nozzle. Using a new nozzle design, coherent liquid jets with chosen diameters between 0.4 and 3.2 mm can be produced over a wide velocity regime ranging from 80 to 800 m sec^{-1} [10]. For all velocities the "head" of the jet is smooth and uniformly curved. These jets can therefore be used to simulate rain drop impact. A more extensive justification for the use of jets to simulate drop impact can be found in earlier publications [11, 12]. The orifice diameter chosen for the present work was 0.8 mm; jets produced with this nozzle simulate the impact of 4 mm diameter drops.

The zinc sulphide specimens were supplied in the form of discs (50 mm diameter and 3.0 mm thick). Only 25 commercially polished specimens were available for the experiments. Before impact the specimens were bonded and acoustically matched to a rigidly mounted 10 mm thick zinc sulphide specimen in order to reduce the effect of reflected stress waves on the impact damage.

A hydraulic bursting technique described earlier [13, 14] was used to measure the fracture stress of specimens after single impact and to quantify the impact damage.

3. Results

3.1. Residual strength measurements

The residual strength of zinc sulphide specimens after liquid jet impact was measured with the hydraulic pressure tester. To determine the initial strength of the specimens eight unimpacted specimens were tested. The average fracture stress of the unimpacted specimens was 68 MPa with a mean standard deviation of 5 MPa. This average initial fracture stress is considerably lower than the value of 100 MPa reported by Adler and Hooker [15]. This low initial fracture stress suggests that the surface finish of the specimens, as supplied, was not very good (as will be confirmed by impact damage features on some of the specimens). No relation between the position of the flaws leading to failure and the "pebble" structure was found.

The fracture stress of impacted zinc sulphide specimens is plotted in Fig. 2 as a function of the impact velocity. No reduction in strength nor visible damage was observed at and below an impact velocity of 125 m sec^{-1} for the eight speci-

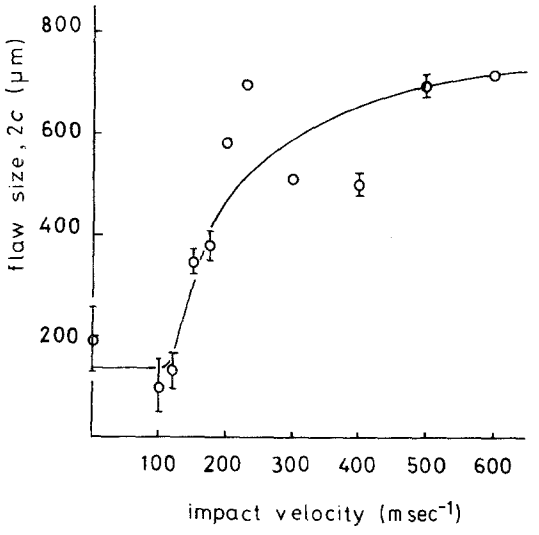

Figure 2 "Residual strength" curve for zinc sulphide for single impact with jets from a 0.8 mm nozzle.

mens tested in this region. Combination of these results with those for unimpacted specimens gives a new average fracture stress for undamaged specimens of 76 MPa. For specimens impacted at 150 to 600 m sec^{-1} the fracture stress was always lower than the initial value. The decrease in fracture stress is particularly large over the velocity range 125 to 175 m sec^{-1}. In the range 200 to 600 m sec^{-1} the residual strength still decreases continuously with impact but at a much lower rate.

Following Matthewson and Field [14] the measured fracture stress, σ_f, was used to calculate the size of the flaw, c, leading to failure using

$$c = 0.75 K_{Ic}^2/\sigma_f^2, \quad (1)$$

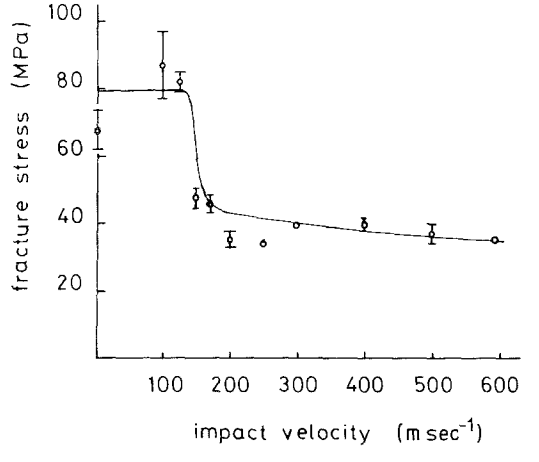

Figure 3 Equivalent flaw sizes for zinc sulphide as a function of the impact velocity (same data as for Fig. 2).

which assumes a semi-circular crack geometry. The calculated equivalent flaw sizes are plotted in Fig. 3 as a function of the impact velocity.

3.2. Surface damage description

3.2.1. 175 m sec^{-3} impact velocity

The impact damage at 175 m sec^{-1} is shown in Fig. 4 and consists of a ring of short circumferential cracks around an undamaged central zone. The ring cracks are shown in more detail in Fig. 4c and d. The residual fracture stress of this specimen was 49.0 MPa wjth an equivalent flaw size of 350 μm. By examining the specimen after fracture in the pressure tester (Fig. 4e and f), the flaw which led to failure could be found (arrowed in Fig. 4a). This flaw is at the outer edge of the damaged zone. The measured crack length, 300 μm, agrees well with the calculated equivalent flaw dimension.

3.2.2. 200 m sec^{-1} impact velocity

The damage due to a 200 m sec^{-1} jet is shown in Fig. 5. The dimensions of the damaged zone have increased in comparison with those in the previous impact. More important, however, is the propagation of two severe pre-existing surface flaws. The damage around one of them is shown in more detail in Fig. 5c and d. Upon testing, a very low fracture stress of 31.2 MPa was obtained for this specimen due to these large defects as shown in Fig. 5e and f. The long defects observed in this specimen are very similar to those observed on zinc sulphide specimens obtained from other sources in which the unidirectionality of the flaws suggested that the flaws were due to the grinding process. During subsequent polishing the griding damage was apparently insufficiently removed. Such a mechanism would also explain the large scatter in the fracture stress for undamaged specimens observed here.

3.2.3. 300 m sec^{-1} impact velocity

At 300 m sec^{-1} the impact damage is as shown in Fig. 6. The impacted area was free from major defects, resulting in a symmetric damage pattern. Both the crack density in the ring around the central zone and the extent of the damaged zone have increased. Comparison of the transmission optical micrographs (Fig. 6a and c) and the reflection micrographs (Fig. 6b and d) shows that material removal due to radial jetting of the jet only occurs in a relatively small region of the

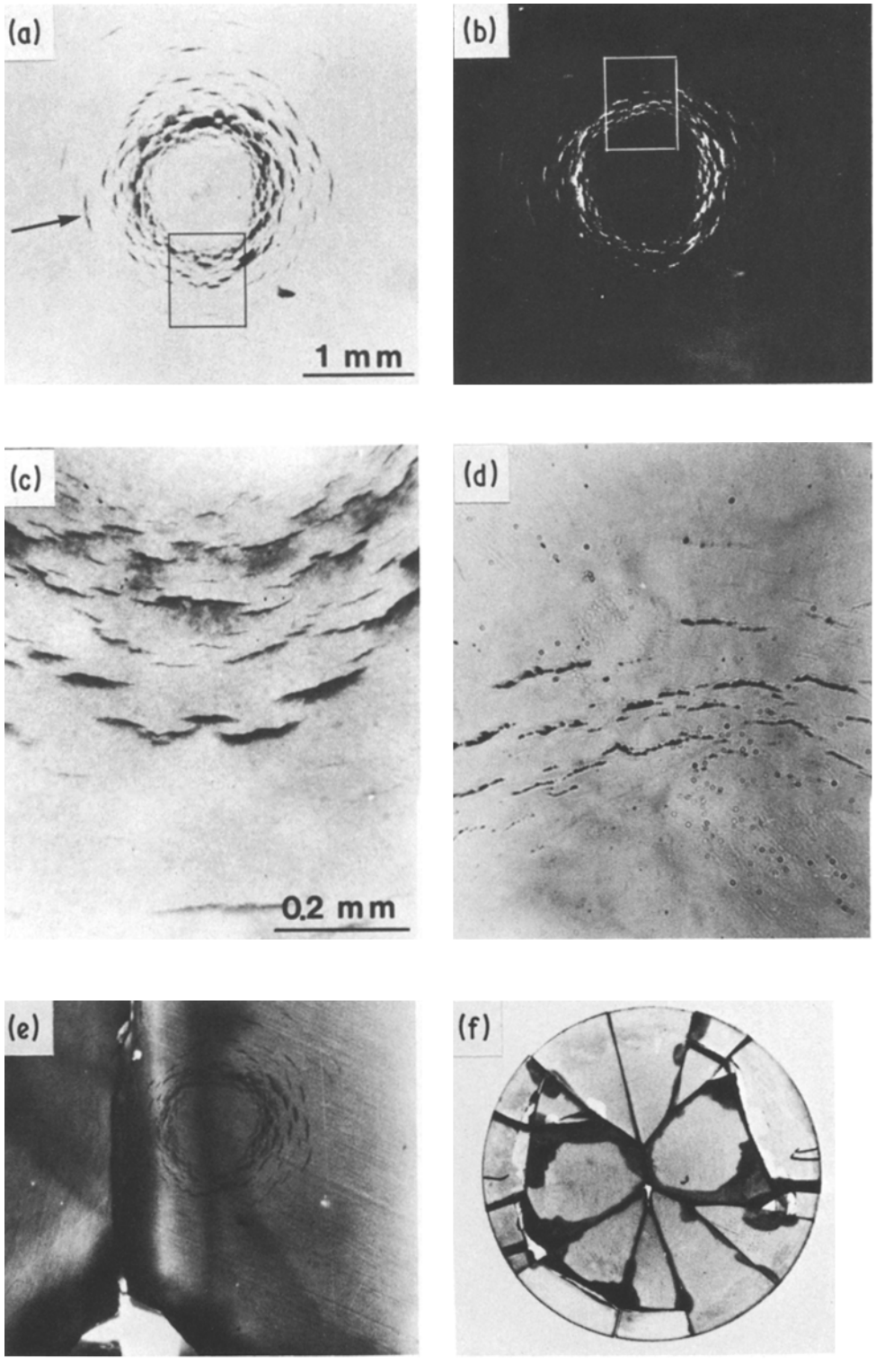

Figure 4 Micrographs obtained with a 0.8 mm jet impact at 175 m sec^{-1}. (a) Optical transmission micrograph of the impact damage. (The flaw leading to failure in the pressure tester is arrowed.) (b) Micrograph with oblique reflective illumination; magnification as in (a). (c) and (d) Enlargements of the areas marked in (a) and (b) respectively; magnification for (d) as in (c). (e) and (f) The specimen after failure in the pressure tester.

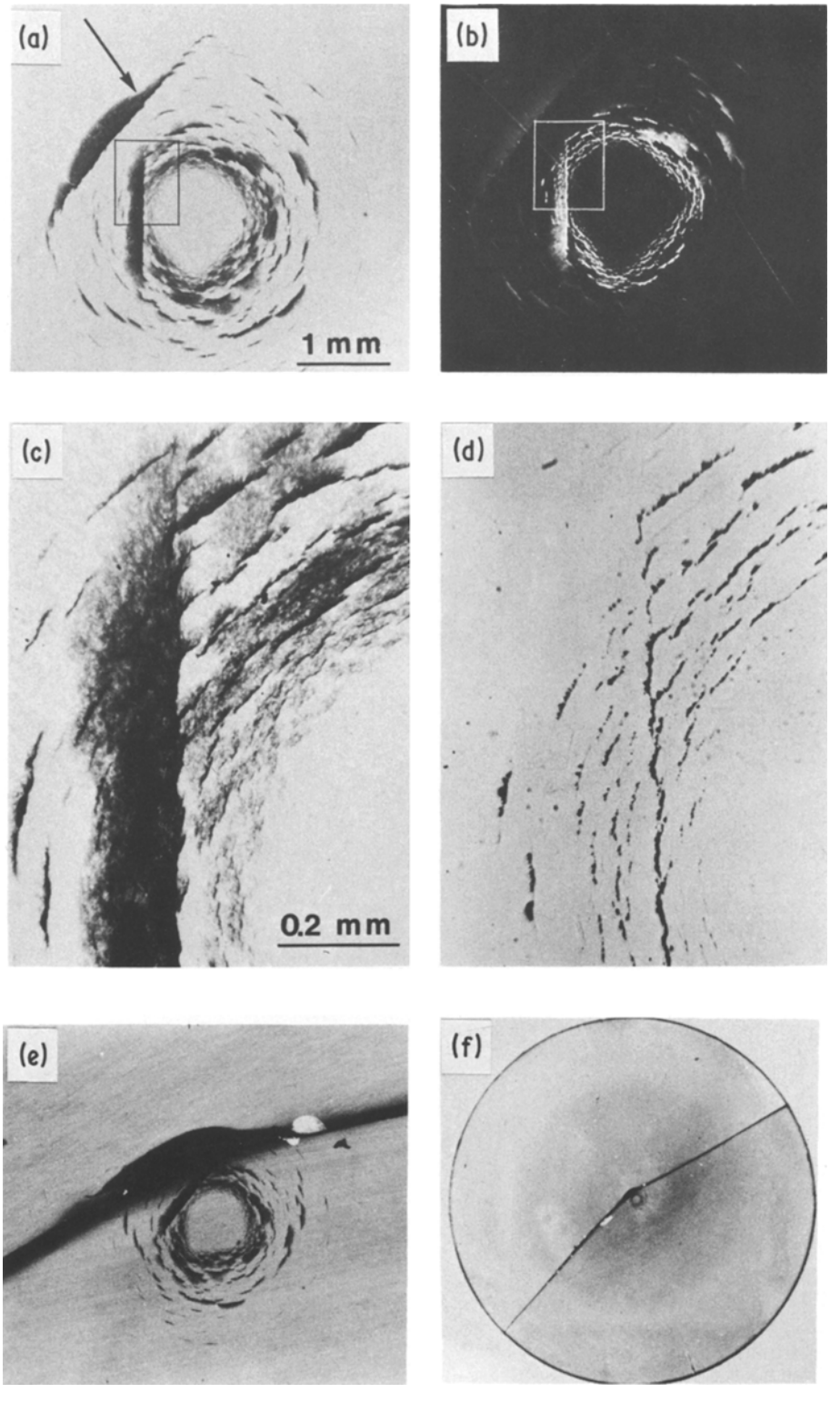

Figure 5 Micrographs obtained with a 0.8 mm jet impact at 200 m sec^{-1}. (a) Optical transmission micrograph of the impact damage. (The flaw leading to failure in the pressure tester is arrowed.) (b) Micrograph with oblique reflective illumination; magnification as in (a). (c) and (d) Enlargements of the areas marked in (a) and (b) respectively; magnification for (d) as in (c). (e) and (f) The specimen after failure in the pressure tester.

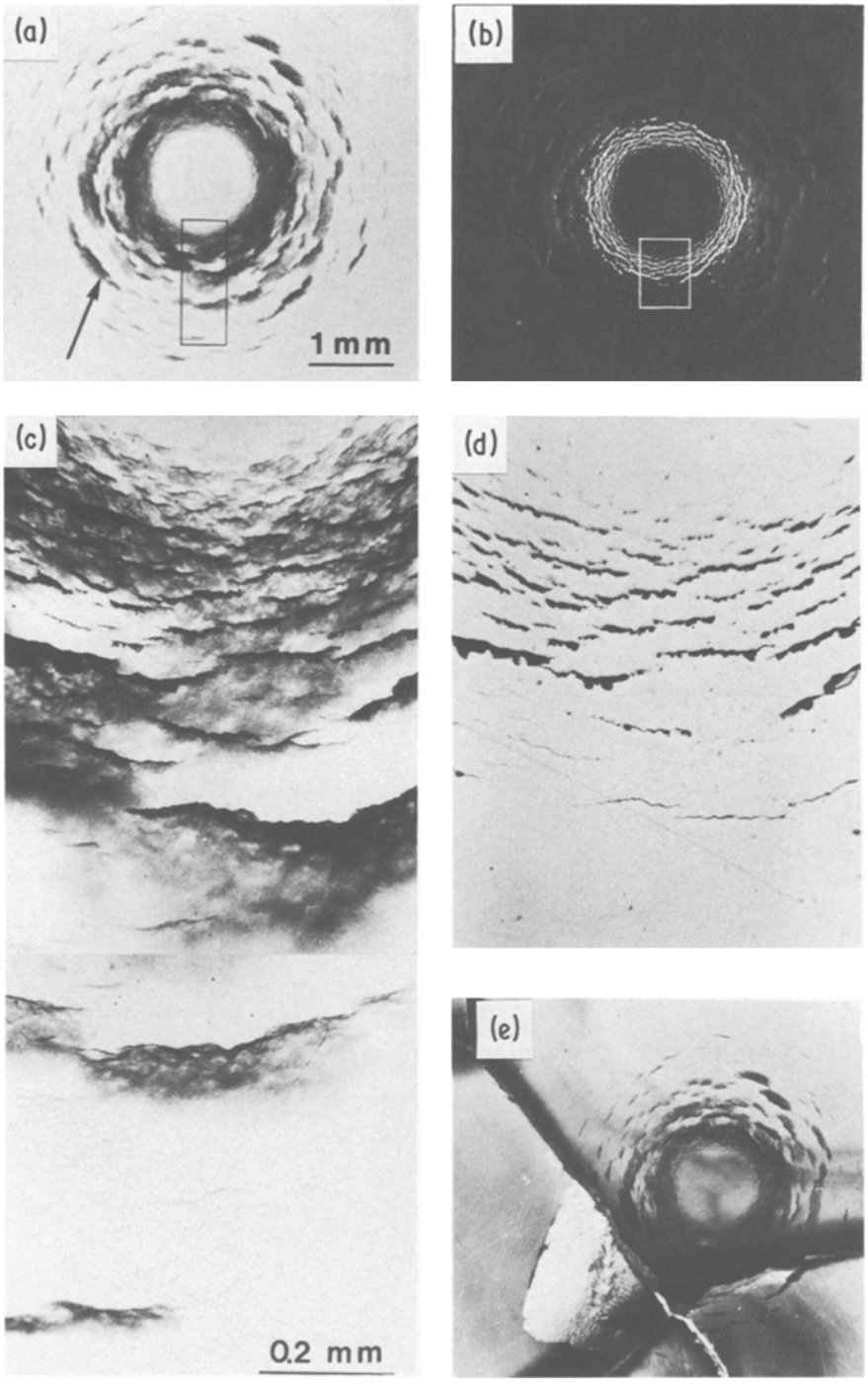

Figure 6 Micrographs obtained with a 0.8 mm jet impact at 300 m sec^{-1}. (a) Optical transmission micrograph of the impact damage. (The flaw leading to failure in the pressure tester is arrowed.) (b) Microcraph with oblique reflective illumination; magnification as in (a). (c) and (d) Enlargements of the areas marked in (a) and (b) respectively; magnification for (d) as in (c). (e) The specimen after failure in the pressure tester.

damaged area. Again a crack at the outer edge of the damaged zone (arrowed in Fig. 6a) has led to failure of the specimen during testing. The calculated equivalent flaw size agrees reasonably well with the observed flaw dimension.

3.2.4. 500 m sec^{-1} impact velocity

Fig. 7 shows the damage after a single jet impact at 500 m sec^{-1}. Both the total damaged area and the crack density have increased considerably in comparison with the 300 m sec^{-1} impact. The increase is particularly clear in Fig. 7c and d. This specimen contained a serious flaw in the impacted area, causing gross material removal.

3.3. Cross-sectional studies

Cross-sectional studies of impact sites for 0.8 mm jets at different impact velocities were made to determine the crack profile into the bulk of the specimen.

3.3.1. 175 m sec^{-1} impact velocity

A top and cross-sectional view through the centre of a 175 m sec^{-1} jet impact is shown in Fig. 8a. The innermost cracks, closest to the central undamaged zone, are very short and approximately straight. The angle between the cracks and the surface is about 80°. Progressing radially outwards, the depth of the cracks gradually increases and the inclination angle of the cracks decreases. The interaction of the Rayleigh wave with a major surface defect on the left of the impact site not only caused significant extension on the surface but also considerable crack growth into the bulk.

3.3.2. 300 m sec^{-1} impact velocity

The features displayed at this impact site (Fig. 8b) are essentially the same as for the 175 m sec^{-1} impact although the cracks have increased both in number and in depth. The innermost cracks tend to curve inwards. Cracks in the middle of the damaged zone are curved outwards. Double crack curvature has also been observed. The outermost cracks are normal to the surface.

3.3.3. 400 m sec^{-1} impact velocity

The damage due to a 400 m sec^{-1} jet impact is shown in top and cross-sectional view in Fig. 8c. The depth of the cracks in the ring zone has further increased. The curvature of the cracks is more pronounced than for the 300 m sec^{-1} jet impact but is essentially the same.

3.3.4. 600 m sec^{-1} impact velocity

Fig. 8d shows the damage due to a 600 m sec^{-1} jet impact on an unsupported 3 mm thick zinc sulphide specimen. The stress wave reflection on the free bottom surface has caused cracking at the rear surface (spalling). The reflected stress waves also interacted with the deepest cracks nucleated at the impacted surface. This has led to cracks below the centre of the impact parallel to the free surface. The cracks nucleated at the surface are similar to those discussed previously. Fig. 8d shows that jet impact damage is not only determined by the impact velocity but also by the specimen dimensions, in particular the specimen thickness.

4. Discussion

It has been shown that the impact of liquid jets from a 0.8 mm diameter nozzle leads to a significant reduction in the residual fracture stress of zinc sulphide specimens for impact velocities in excess of 125 m sec^{-1}. In earlier research, Field *et al.* [12], attempted to correlate jet and drop impact damage. They have shown that jet and drop impact in polymethylmethacrylate consists of a central plateau of undamaged material surrounded by an annular depression. Their equivalence relation, which is based on the diameter of this undeformed zone, predicts that jets from a 0.8 mm nozzle simulate the impact of 4 mm diameter drops over a wide velocity regime. It should be pointed out that this equivalence relation might be target material dependent. In particular, in the case of brittle materials the size and number of impact induced cracks could be more suitable parameters for comparing drop and jet impacts. Initial experiments to establish the jet-drop equivalence relation on this basis [16], however, also suggest that the jets used simulate ~4 mm drop impacts. This equivalence value can now be used to estimate the threshold velocity for standard 2 mm drop impacts using the relation proposed by Rickerby [17]:

$$\frac{V_a}{V_b} \simeq \left(\frac{r_a}{r_b}\right)^{1/2} \tag{2}$$

where V_a, r_a and V_b, r_b are the threshold velocity and drop radius for conditions a and b, respectively. The above equation was derived by considering the criteria for dynamic crack growth [18] and the relation between the duration of the high-pressure stage and the radius of the

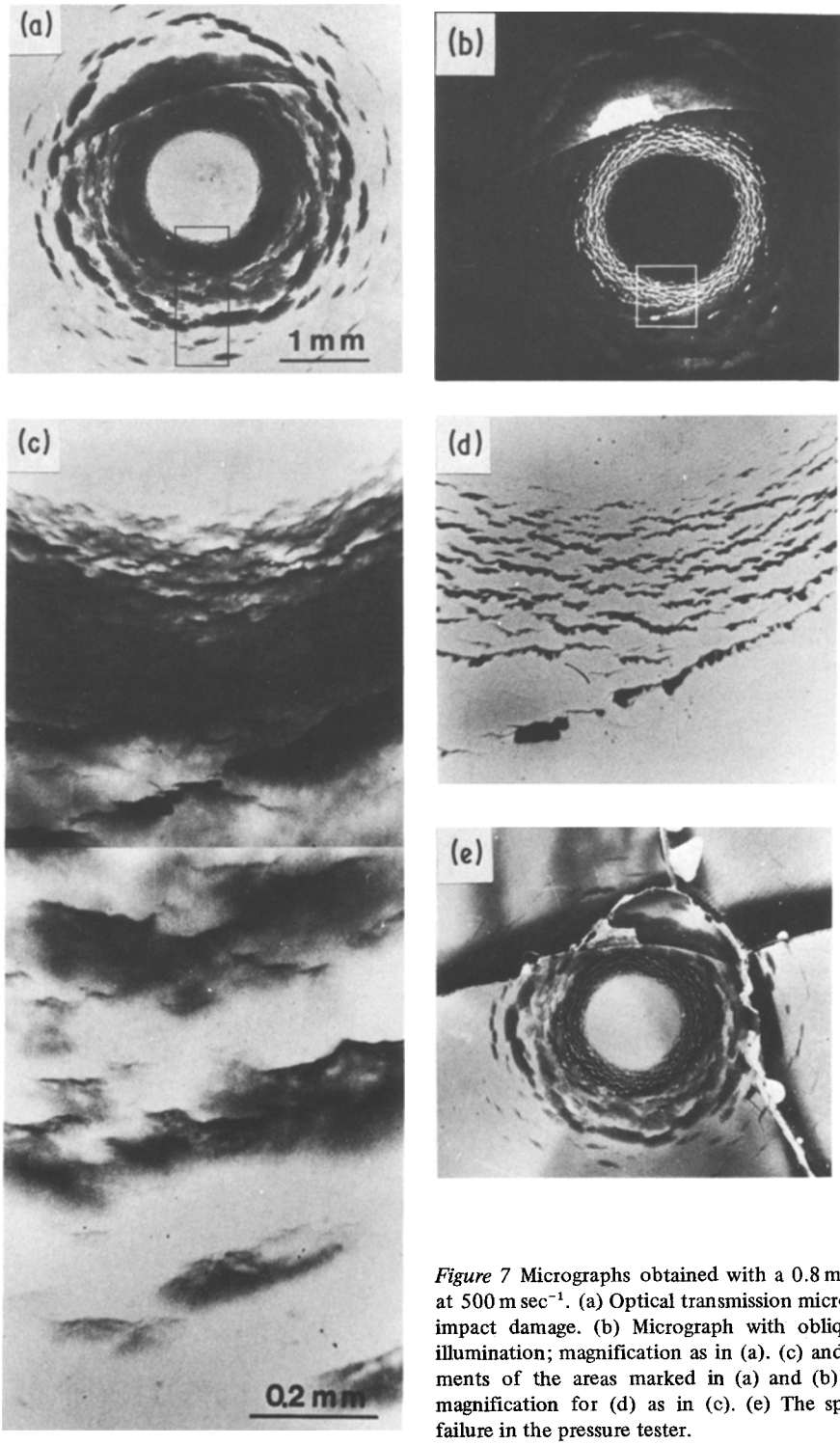

Figure 7 Micrographs obtained with a 0.8 mm jet impact at 500 m sec^{-1}. (a) Optical transmission micrograph of the impact damage. (b) Micrograph with oblique reflective illumination; magnification as in (a). (c) and (d) Enlargements of the areas marked in (a) and (b) respectively; magnification for (d) as in (c). (e) The specimen after failure in the pressure tester.

impacting drop or jet [11]. Using this equation a threshold velocity for 2 mm drop impacts of 175 ± 5 m sec^{-1} is predicted. Such a value is in good agreement with the results of Hackworth and Kocher [19] who reported a threshold velocity for a 2 mm drop impact of 175 m sec^{-1} using a whirling-arm installation. It should be mentioned here that multiple jet impact experiments on soda-lime glass [20] have shown that the threshold velocity depends only weakly on the number of impacts.

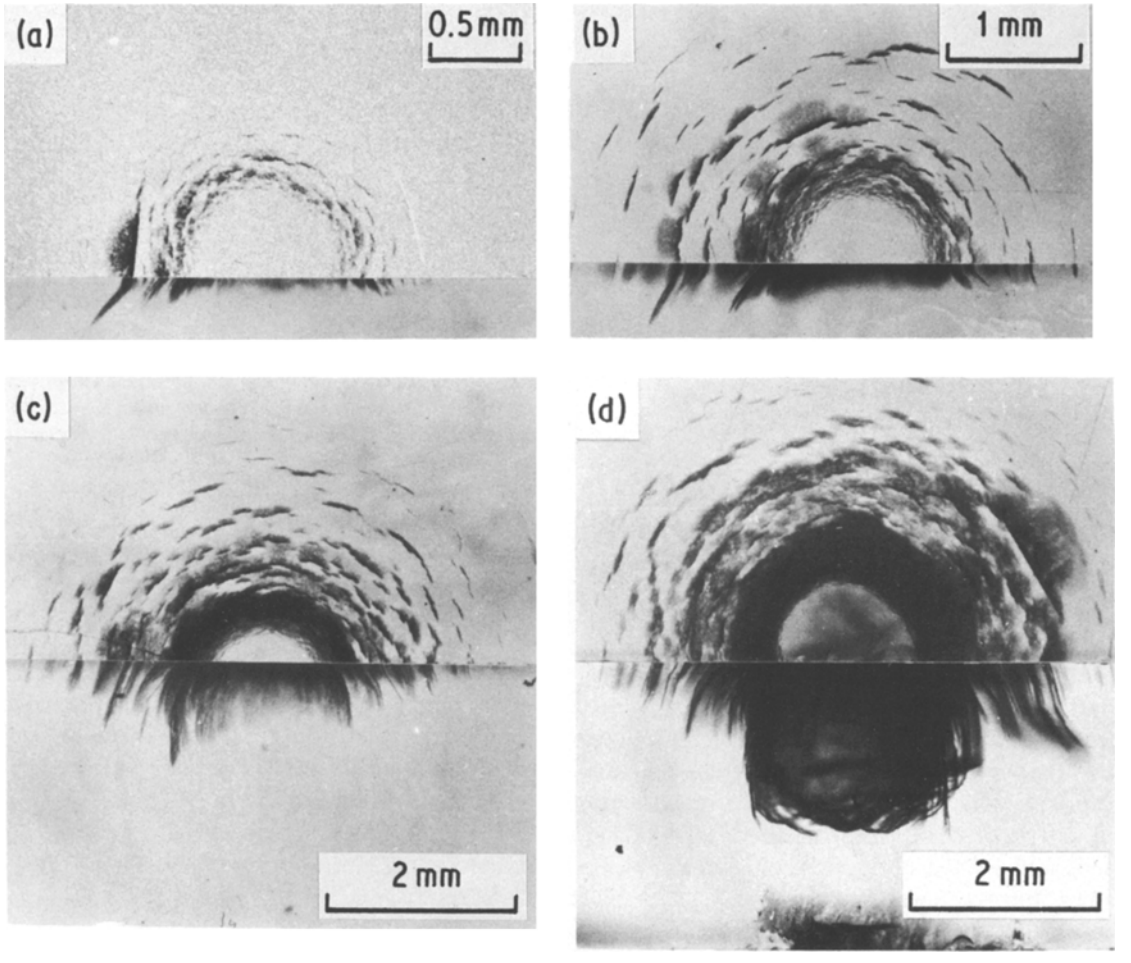

Figure 8 Cross-sections of the 0.8 mm jet impact damage in zinc sulphide. (a) 175 m sec^{-1}, (b) 300 m sec^{-1}, (c) 400 m sec^{-1}, (d) 600 m sec^{-1}.

The jet impact damage in zinc sulphide consists of a ring of short circumferential cracks around an undamaged central zone. These cracks are due to the interaction between the Rayleigh surface wave generated during the initial stages of the impact, when the liquid behaves compressibly, and pre-existing defects. Within the ring the average size of the cracks increased with radial distance from the centre of the impact but their density decreases. This variation is due to the changes in the amplitude and duration of the Rayleigh wave with radial distance: initially the wave amplitude is very high but its duration is extremely short (< 0.1 μsec). Using a simple dynamic fracture mechanics model [20], it can be shown that under these conditions a very small initial flaw size is sufficient to cause crack growth but that the amount of growth is small because of the short duration of the pulse. When the Rayleigh wave expands outwards its amplitude decreases but its duration increases. A larger initial flaw size is now required for the stress pulse to exceed K_{Ic} at the crack tip but when this happens a considerable amount of crack growth will occur. Therefore, the largest and most serious flaws will almost always be found at the outer edge of the damaged zone. At very large distances the stress pulse amplitude has decreased so much that none of the defects surrounding the impact site will grow.

Examination of the damage features has shown that in this material there are two types of pre-existing defects: a high density of very small defects, which are responsible for the large number of relatively small cracks in the damaged area, and much rarer large defects, which lead to very large final crack sizes. While the second type of defects are due to grinding, polishing and handling damage, the first type of defects seems to be related to

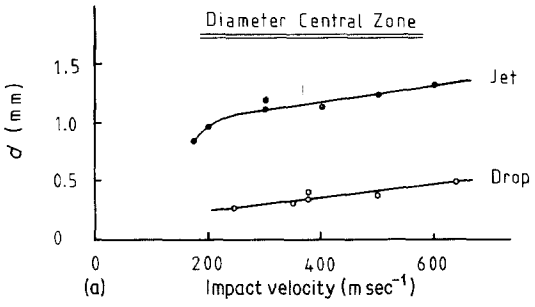

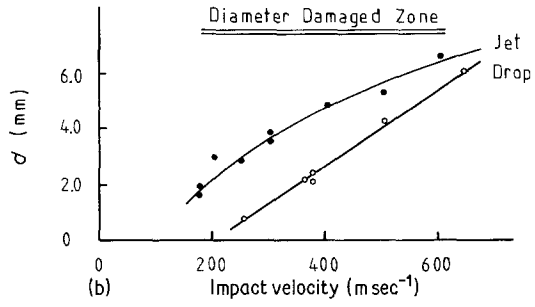

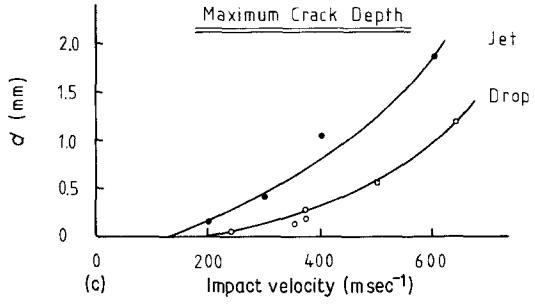

Figure 9 Velocity dependence of the impact damage parameters. (a) Shows the diameter of the undeformed zone for jets and drops; (b) shows the maximum diameter of the damaged zone for jets and drops; and (c) shows the maximum crack depth for jets and drops. (Data for 2 mm drop impact damage from Adler [21]. Equivalent drop size for jet predicted as ~ 4 mm.)

the grain size. For the fine-grained material examined here, the average initial flaw size will be small but their density high. It can be shown with the theroretical model for the residual strength curve described elsewhere [20] that a high density of defects of almost identical size leads to a sharp and well-defined drop in the residual fracture stress for specimens impacted at velocities just above the threshold velocity, as indeed observed. In the case of soda-lime glass the defect density is lower and the variation in the initial defect size much larger so that the drop in the residual fracture stress occures over a much wider velocity range [20]. It can now be argued that the threshold velocity for rain erosion damage will depend on the grain size: the smaller the grain size, the smaller the initial defect size and the higher the stress pulse amplitude (and therefore impact velocity) required for crack growth. Although the effect of the grain size on the rain erosion damage in zinc sulphide has not yet been studied, Hackworth and Kocher [19] have shown that for CVD zinc selenide the rain erosion resistance increases considerably with decreasing grain size.

The impact damage on zinc sulphide can conveniently be characterized by three parameters: (a) the diameter of the undeformed zone, (b) the diameter of the damaged area, i.e. the area containing all circumferential cracks, and (c) the maximum crack depth. These parameters have been used to compare jet and drop impact damage. The drop impact experiments were performed by Adler and co-worker [21, 22]. In their very realistic but complex rain impact simulation experiments a sabbot, containing the zinc sulphide specimen, impacts an unsuspended 2 mm diameter water drop. After impact the sabbot is brought to rest without introducing additional damage to the impacted specimen.

The velocity dependence of the diamter of the central zone is plotted in Fig. 9a for the two types of impact. Taking into account that the jet simulates a larger drop size, the agreement is good. It should be added that the diameter for drop impact was measured after an etching treatment. The apparent diameter of the undamaged zone was about 25% smaller after etching. The diameter of the undeformed zone for a jet impact is just over twice that for a 2 mm diameter drop impact. This agrees with our suggestion that we simulate an approximately 4 mm diameter drop impact with our 0.8 mm jet impact. It also agrees with the prediction of Bowden and Field [11] that, at a particular velocity, the size of the central region is proportional to the drop radius.

The diameter of the damaged zone is shown in Fig. 9b for drop and jet impact. A good agreement is obtained. However, at high velocities the diameter of the damaged zone seems to increase more rapidly for drop impact. Although the results have to be treated with caution, since the size of the damaged zone depends strongly on the size and distribution of the pre-existing defects, this might be a genuine effect. In the later stages of the impact there are differences in the pressure distribution for drops and jets and these differences

become more important at high velocities. In the case of drops, high pressures are applied over a larger area, resulting in more extensive damage. This explanation is confirmed by a rather limited number of 0.4 mm jet impacts (which simulate 2 mm drop impacts) on similar zinc sulphide specimens as used for drop impacts. The best agreement in the diameter of the damaged area was obtained at impact velocities of 300 and 400 m sec^{-1}. For a 600 m sec^{-1} impact however, the damage produced by drop impact was considerably more extensive and particularly at larger distances from the centre of impact [22].

The maximum depth of the cracks as a function of the impact velocity is plotted in Fig. 9c for drop and jet impacts. The same velocity dependence is obtained for two conditions. Fig. 9c shows rather clearly the effect of "drop" dimensions on the threshold velocity for impact damage.

Finally, it should be stressed that we do not claim a complete agreement between jet and drop impact damage. Due to the differences in the loading condition, in particular in the flow pattern of the liquid over the surface, there are differences in the exact profile of the cracks, the deformation in the central undamaged zone and the extent of the damage. However, the present work has shown that the very simple and inexpensive jet technique can be used to obtain a good estimate of drop impact damage over a wide velocity regime.

5. Conclusions

The pattern of jet-impact damage in zinc sulphide is characteristic of that in brittle materials and consists of a central undamaged region surrounded by an annulus of short circumferential cracks. The size of this damaged zone increases with the impact velocity. The cracks form at pre-existing defects and are developed by the Rayleigh surface wave generated by the impact. Within the annular damaged zone the average crack length increases with radial distance from the centre of the impact but the number of cracks decreases. These changes are due to the increase in the duration of the Rayleigh wave while propagating outwards, and to the simultaneous decrease in pulse amplitude, respectively.

The defect distribution in zinc sulphide consists of two different types of defects: a large number of small defects which may be related to or controlled by the grain size, and some large defects caused by the surface preparation. Although the samples, as received, appeared to have an excellent surface finish, the large cracks which formed in some specimens following impact suggest that not all the grinding damage had been removed during the subsequent polishing stages. For relatively weak materials, such as zinc sulphide, careful surface preparation is shown to be essential.

The shape of the "residual strength" curve for zinc sulphide is similar to those reported earlier for other brittle materials [10, 14, 20]. There is an initial plateau up to a critical threshold velocity, where the specimen retains its strength. This is followed by a region in which the post-impact strength drops rapidly, after which the fracture stress decreases only slowly. Other work [20] has shown that the threshold velocity itself decreases only slightly with the number of impacts so that the threshold velocity obtained in single impact experiments has practical value. For the material studied, a threshold velocity of 125 m sec^{-1} was observed for impacts with 0.8 mm jets, which are equivalent to ~ 4 mm diameter drops for most of the velocity range studied [12, 17]. We estimate from this a critical velocity for impact damage due to 2 mm diameter drop impacts of 175 ± 5 m sec^{-1}.

The damage produced by jet and drop [21, 22] impact has been compared. Although the simulation of drop impact by our jets is not perfect, the technique clearly reproduces the damage mechanisms and the practically important threshold velocity. The advantages of the jet technique are significant, since it is simple, inexpensive and can be used to simulate drop impact over a wide range of drop sizes and impact velocities.

Acknowledgements

We thank Dr M. J. Matthewson and Dr N. S. Corney for comments on the manuscript. The research was supported in part by the Ministry of Defence (Procurement Executive) and by the US Air Force of Scientific Research, under Grant number 78–3705.

References

1. K. J. MARSH and J. A. SAVAGE, *Infrared Phys.* **14** (1974) 85.
2. J. A. SAVAGE and S. NIELSEN, *ibid.* 5 (1965) 195.
3. I. W. DONALD and P. W. McMILLAN, *J. Mater. Sci.* **13** (1978) 1151.
4. *Idem, ibid.* **13** (1978) 2301.
5. F. P. BOWDEN and J. H. BRUNTON, *Proc. Roy. Soc.* **A263** (1961) 443.
6. B. R. LAWN and E. R. FULLER, *J. Mater. Sci.* **10**

(1975) 2016.
7. D. P. WILLIAMS and A. G. EVANS, *J. Test. Eval.* **1** (1973) 264.
8. G. F. SCHMITT, private communication (1977).
9. W. F. ADLER and S. V. HOOKER, *J. Mater. Sci.* **13** (1978) 1015.
10. J. E. FIELD, D. A. GORHAM, J. T. HAGAN, M. J. MATTHEWSON, M. V. SWAIN and S. VAN DER ZWAAG, Proceedings of the 5th International Conference on Erosion by Solid and Liquid Impact, Cavendish Laboratory, Cambridge (1979) paper 13.
11. F. P. BOWDEN and J. E. FIELD, *Proc. Roy. Soc.* **A282** (1964) 331.
12. J. E. FIELD, D. A. GORHAM and D. G. RICKERBY, Proceedings of the ASTM Conference on Erosion, Vail, Colorado, October, 1977, edited by E. F. Adler (ASTM, Philadelphia, PA, USA, 1979) p. 298.
13. D. A. GORHAM and D. G. RICKERBY, *J. Phys.* **E8** (1975) 794.
14. M. J. MATTHEWSON and J. E. FIELD, *ibid.* **E13** (1980) 355.
15. W. F. ADLER and S. V. HOOKER, *Wear* **48** (1978) 103.
16. P. W. BLAIR, PhD thesis, University of Cambridge (1982).
17. D. G. RICKERBY, PhD thesis, University of Cambridge (1977).
18. B. STEVERDINGH and S. H. LEHNIGK, *Ceram. Bull.* **49** (1970) 1057.
19. J. V. HACKWORTH and L. H. KOCHER, Report No. AFML-TR-78-184 (Bell Aerospace, Buffalo, 1978).
20. S. VAN DER ZWAAG and J. E. FIELD, *Eng. Fract. Mech.* in press.
21. W. F. ADLER, Report No. Cr 79-611 (Effects Technology Inc., Santa Barbara, 1979).
22. W. F. ADLER and T. W. JAMES, Report No. CR 80-758 (Effects Technology Inc., Santa Barbara, 1980).

Received 22 December 1981
and accepted 1 February 1982